



<b>Publication Year</b>	2018
<b>Acceptance in OA @INAF</b>	2020-11-06T10:56:37Z
<b>Title</b>	Modeling the JANUS stray-light behavior
<b>Authors</b>	GREGGIO, DAVIDE; Munari, M.; MAGRIN, DEMETRIO; Paolinetti, R.; Barilli, M.; et al.
<b>DOI</b>	10.1117/12.2313204
<b>Handle</b>	<a href="http://hdl.handle.net/20.500.12386/28182">http://hdl.handle.net/20.500.12386/28182</a>
<b>Series</b>	PROCEEDINGS OF SPIE
<b>Number</b>	10698

# PROCEEDINGS OF SPIE

[SPIDigitalLibrary.org/conference-proceedings-of-spie](https://spiedigitallibrary.org/conference-proceedings-of-spie)

## Modeling the JANUS stray-light behavior

D. Greggio, M. Munari, D. Magrin, R. Paolinetti, M. Barilli, et al.

D. Greggio, M. Munari, D. Magrin, R. Paolinetti, M. Barilli, A. Turella, M. Zusi, V. Della Corte, P. Palumbo, R. Mugnuolo, M. Amoroso, M. Castronuovo, R. Ragazzoni, "Modeling the JANUS stray-light behavior," Proc. SPIE 10698, Space Telescopes and Instrumentation 2018: Optical, Infrared, and Millimeter Wave, 106984V (6 July 2018); doi: 10.1117/12.2313204

**SPIE.**

Event: SPIE Astronomical Telescopes + Instrumentation, 2018, Austin, Texas, United States

# Modeling the JANUS stray-light behavior.

D. Greggio<sup>\*a</sup>, M. Munari<sup>b</sup>, D. Magrin<sup>a</sup>, R. Paolinetti<sup>c</sup>, M. Barilli<sup>c</sup>, A. Turella<sup>c</sup>, M. Zusi<sup>d</sup>, V. Della Corte<sup>e, d</sup>, P. Palumbo<sup>e, d</sup>, R. Mugnuolo<sup>f</sup>, M. Amoroso<sup>f</sup>, M. Castronuovo<sup>f</sup>, R. Ragazzoni<sup>a</sup>

<sup>a</sup>INAF – Osservatorio Astronomico di Padova, Vicolo dell'Osservatorio 5, 35122 Padova, Italy

<sup>b</sup>INAF – Osservatorio Astrofisico di Catania, Via S.Sofia 78, 95123 Catania, Italy

<sup>c</sup>Leonardo, Via Einstein35, 50013 Campi Bisenzio (FI), Italy

<sup>d</sup>Istituto di Fisica e Planetologia Spaziali (IAPS), Roma, Italy

<sup>e</sup>Dipartimento di Scienze e Tecnologie, Università degli Studi di Napoli "Parthenope", Napoli, Italy

<sup>f</sup>ASI Centro di Geodesia Spaziale, Località Terlecchia, 75100 Matera (MT), Italy

## ABSTRACT

JANUS is the camera of the ESA mission JUICE, dedicated to high-resolution imaging in the extended-visible wavelength region (340 – 1080nm). The camera will observe Jupiter and its satellites providing detailed maps of their surfaces and atmospheres. During the mission, the camera will face a huge variety of observing scenarios ranging from the imaging of the surfaces of the satellites under varying illumination conditions to limb observation of the atmospheres. The stray-light performance of JANUS has been studied through non-sequential ray-tracing simulations with the aim to characterize and optimize the design. The simulations include scattering effects produced by micro-roughness and particulate contamination of the optical surfaces, the diffusion from mechanical surfaces and ghost reflections from refractive elements. The results have been used to derive the expected stray-light performance of the instrument and to validate the instrument design.

**Keywords:** space mission, Jupiter, JUICE, stray-light, radiometry, scattering

## 1. INTRODUCTION

JANUS (Jovis Amorum ac Natorum Undique Scrutator) is an optical camera for the JUICE (JUPiter ICy moons Explorer) satellite, the large L class mission under development by ESA<sup>1,2</sup>. JUICE is devoted to the detailed study of Jupiter and its moons, in particular Europa and Ganymede. The JUICE space mission is planned for launch in 2022 and arrival at Jupiter in 2030, and it will operate for four years, making detailed observations of the Jovian system. The JANUS science objectives are:

- Characterize Ganymede, Callisto, and Europa as planetary bodies, including their potential habitability, with special focus on Ganymede;
- Characterize and study the physical properties of other satellites of the Jupiter system, including Io, the irregular and inner satellites;
- Perform a physical characterization of the ring system;
- Study the external layers (down to the troposphere) of Jupiter's atmosphere;
- Study the magnetosphere in which Jupiter and its satellites are embedded, and the complex interactions taking place in the Jovian system.

\*davide.greggio@inaf.it;

A satisfactory answer to all these questions requires also measurements taken by an imaging system with optimum performance<sup>3,4</sup>. Such a system will have a major role in the mission, not only with its camera-specific scientific results, but also in providing the necessary context for most of the other instruments on-board JUICE as, for instance, the Digital Terrain Model (DTM) of a few regions of Ganymede required by RIME (Radar for Icy Moons Explorations) for its topographic correction<sup>5,6</sup>.

The JANUS camera is a catadioptric telescope observing in the wavelength range 340 – 1080 nm and with a rectangular field of view of 1.3 x 1.7 degrees. The camera will provide detailed observations of Jupiter and its moons, with the possibility to choose among a set of 13 narrowband and broadband filters. JANUS will perform a complete mapping of the surface of Ganymede and will observe extensively the surface and atmosphere of Jupiter, Europa, Callisto and other targets. During the 4-years observing phase, the camera will face a huge variety of observing scenarios ranging from the imaging of the surfaces of the satellites under varying illumination conditions to limb observation of the atmospheres. For this reason, it is mandatory to accurately model, predict and optimize the stray-light performance of the instrument. In this paper, we present the stray-light analysis performed for JANUS in order to assess its radiometric capabilities. The analysis is based on non-sequential ray-tracing simulations with the software FRED. The simulations take into account the effects of ghost reflections from refractive elements, scattering from micro-roughness and particulate contamination of optical surfaces and diffusion from mechanical surfaces. The results obtained are used to identify critical stray-light paths and validate the design/geometry. Moreover, the quantitative analyses performed can be used to predict the stray-light irradiance on the detector for different observing scenarios and to compare it with the instrument scientific requirements.

## 2. OPTO-MECHANICAL MODEL

The Leonardo Company is in charge by the Italian Space Agency (ASI) to develop the opto-mechanical model of JANUS in collaboration with the Italian Institute of Astrophysics (INAF) as the JANUS consortium partner. The optical scheme is derived from a Ritchey-Chrétien telescope and is characterized by aspheric primary and secondary mirrors (up to the 10<sup>th</sup> order aspheric shape) and a field corrector consisting of three lenses in fused silica. A similar design has already been used for other space cameras like the High Resolution Imaging Channel of SIMBIO-SYS<sup>8</sup> in the Bepi Colombo mission or the CHEOPS space mission<sup>9,10</sup> devoted to exoplanet hunting.

The telescope optics are followed by a filter wheel composed by 13 narrow-band, broad-band and panchromatic filters in the 0.34  $\mu\text{m}$  to 1.1  $\mu\text{m}$  range. Finally, a CMOS Imaging Sensor 115 (CIS115) with a 2000 by 1504 pixel array each 7  $\mu\text{m}$  square<sup>11</sup>, records the image with an IFOV of 15 $\mu\text{rad/px}$ . A flat window in front of the detector protects it from external radiation.

The baffling scheme is composed by five baffles:

- 1) An **external baffle** limits the illumination angle from outside. The tube structure is placed towards the outside direction with respect to the secondary mirror. It is characterized by vanes to block first-order stray-light paths from the baffle itself and the diameter and length are optimized to prevent direct illumination of the detector from external sources.
- 2) An extension of the external baffle placed between M1 and M2 (**M1-M2 Tube**) separates the optical path region from the rest of telescope structure.
- 3) A short baffle on the secondary mirror (**M2 baffle**) helps blocking direct illumination from outside together with the external baffle.
- 4) A conical baffle on the primary mirror hole (**M1 baffle**) serves both as a support structure for the corrector and to reduce the solid angle through which the detector sees the region around M2.
- 5) A conical **detector baffle** prevents illumination of the surfaces close to the detector itself and reduces stray-light from sources close to the field of view.

Apart from baffles and optical elements, most of the other components of the telescope structure are neither visible from the detector nor illuminated from outside thus they give a negligible contribution to the stray-light since they can produce only third-order scattering paths. Some exceptions are the spiders supporting M2, the mountings of the optical elements and the lens spacers.

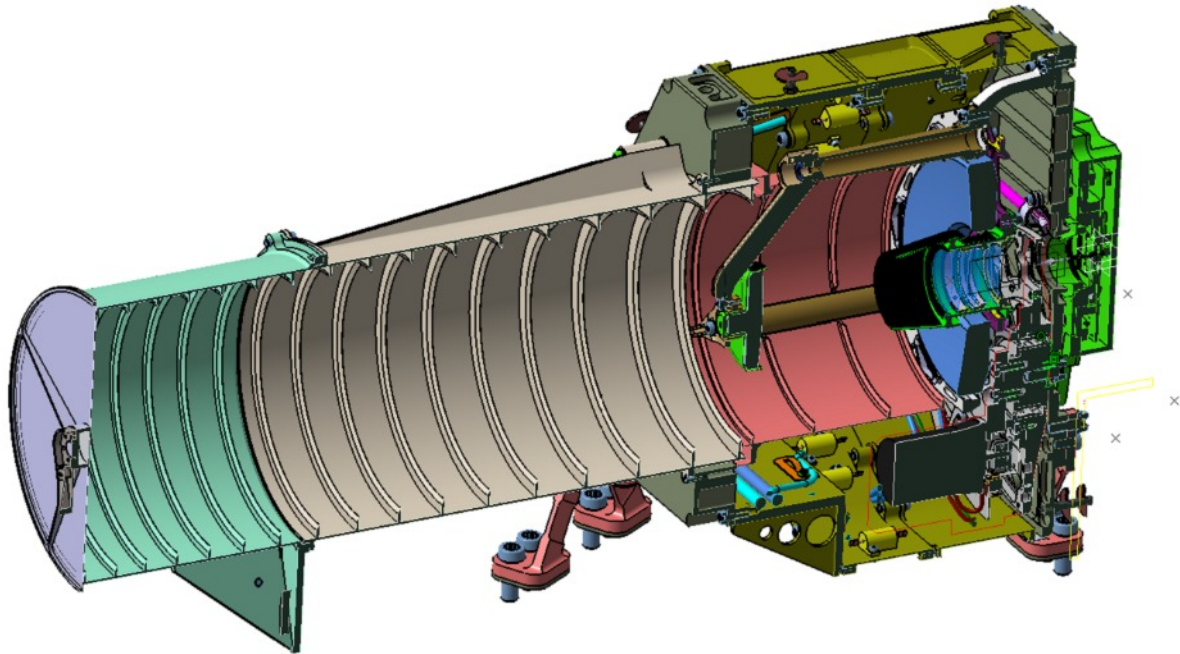


Figure 1. Opto-mechanical layout of JANUS

### 3. STRAY-LIGHT MODEL

#### 3.1 Geometrical model

The stray-light model was developed with the ray-tracing software FRED by Photon Engineering. It is based on a simplified version of the opto-mechanical model. The simplification procedure is based on the identification of illuminated surfaces (i.e. surfaces that can be hit by light coming from outside the telescope) and critical surfaces (i.e. surfaces visible from the detector). First, all the surfaces which were neither critical nor illuminated were discarded. As a second step, the surfaces have been grouped into sub-assemblies and, where possible, their geometry has been simplified and replaced by object primitives available on the software in order to speed-up the ray-trace.

The simplification procedure is critical for many reasons:

1. It allows to speed-up the loading of the model and the ray-trace and reduces ray-trace errors often encountered when importing CAD objects directly into the software.
2. It forces the designer to do a critical review of the components/surfaces before starting the ray-trace
3. It helps to keep the model organized and easily upgradable, for example when the design of some component is changed or a more detailed analysis is required.
4. It allows to set the scattering properties in a straightforward way
5. It allows to set-up the “allowed” ray-trace paths (for instance by using the importance sampling feature available on many stray-light software) more easily.
6. It is fundamental to analyze the results of the analysis and to identify the critical areas of the design.

In the case of JANUS, the telescope sub-assemblies have been organized in a tree structure that can be easily visualized in Figure 2 and Figure 3 , where different colors identify different components. Each branch of the tree is further detailed, up to the level of single surfaces composing each piece.

As a support to the ray-trace, we also identified the size and position of the detector image as seen through part of the optical train (for example through M2 and the corrector). For each detector image we generate a closed curve which is then used to set-up the scattering region of interest for each surface. Doing this, rays are scattered only towards the detector, significantly increasing the efficiency of the simulation and avoiding the generation of irrelevant rays.

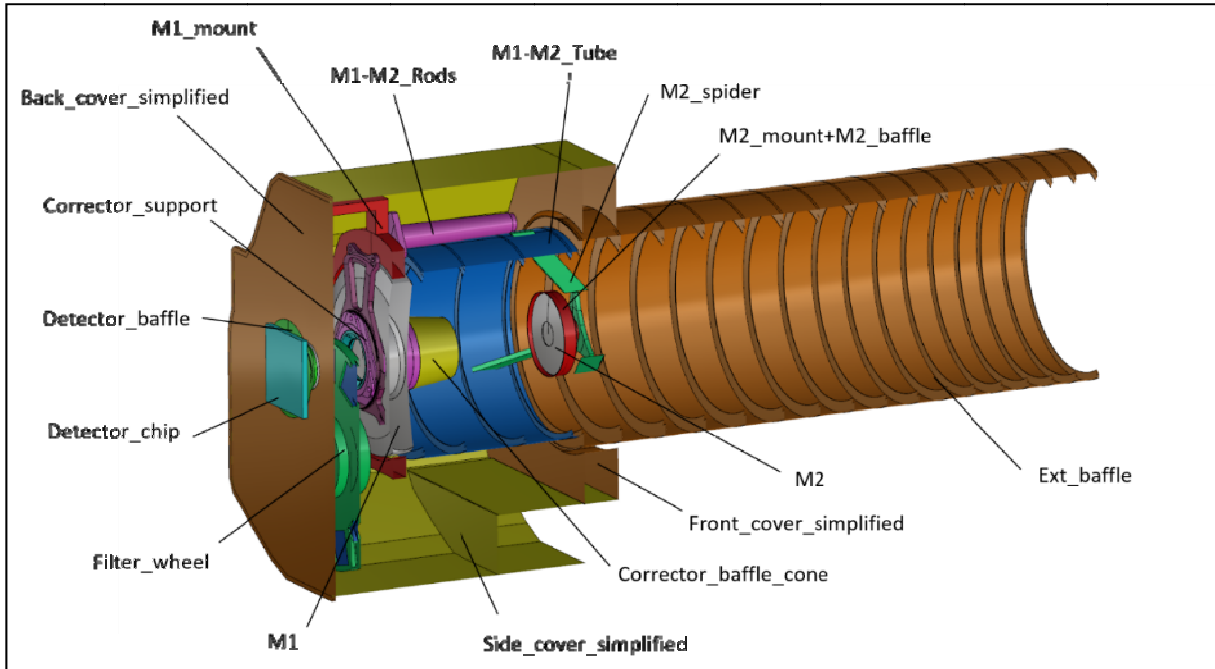


Figure 2. 3D Layout of the FRED simplified model

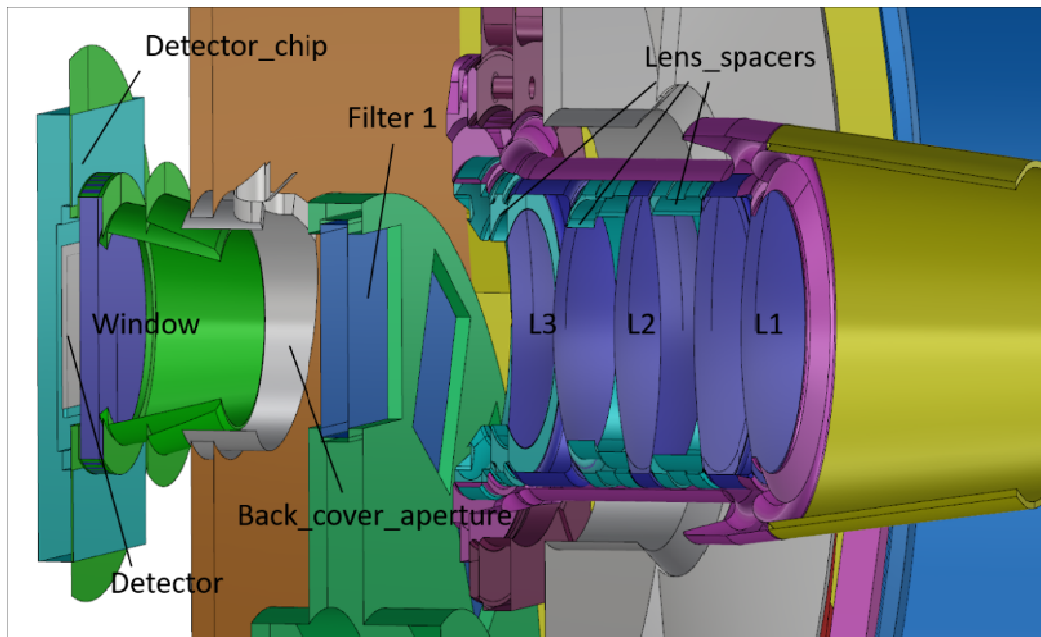


Figure 3. 3D Layout of the FRED simplified model. Detail of the three-lens corrector and detector

### 3.2 Simulation strategy

The stray-light simulation has been divided in two main phases. In the first phase we identified the first-order scattering paths i.e. those paths that are generated by surfaces that are both critical and illuminated. The critical surfaces were identified by doing a backward ray-trace from the detector. The illuminated surfaces were identified by illuminating the entrance aperture of JANUS with a collimated beam covering a grid of entrance directions (polar and azimuth angles). During this qualitative analysis, scattering is not considered: mechanical surfaces are absorptive while optical surfaces are perfectly reflecting or transmitting. Since scattering is not considered the ray-tracing is very fast and allows a very good sampling both in terms of spatial and angular separation of rays. For every illumination angle we then produced a list of surfaces by matching the list of critical and illuminated surfaces and by assigning an estimate of their “criticality” by considering the product between the number of critical rays and the number of illuminating rays incident on that surface. This analysis does not consider the BRDF of the surfaces but allows a fast identification of the critical paths and provides a first feedback for the improvement of the design. Moreover, since the information on the illumination angle is registered, it is possible to identify the angular range in which a particular surface is illuminated which is particularly useful to propose modifications of the baffling scheme or just to determine a set of critical angles to avoid.

The second simulation phase is more quantitative and computationally intensive because it considers the BSDF (Bidirectional Scattering Distribution Function) profile of each surface. In the case of JANUS we consider the scattering produced by mechanics, micro-roughness of optical components and particulate contamination of optical surfaces. We also included ghost reflections by considering the partial reflectivity of glass surfaces.

The stray-light behavior of JANUS is characterized by calculating the Spatial Point Source Transmittance (SPST) of the instrument. SPST is defined as the stray-light irradiance map on the detector generated by illuminating the entrance aperture of the instrument with a collimated source of unit irradiance and it is a function of the entrance angle:

$$SPST(\theta, \varphi, x, y) = \frac{E_{det}(\theta, \varphi, x, y)}{E_{ent}(\theta, \varphi)}$$

Where  $\theta$  is the polar angle with respect to the boresight direction,  $\varphi$  is the azimuth angle,  $x$  and  $y$  are the positions on the detector,  $E_{det}$  is the irradiance on the detector and  $E_{ent}$  is the irradiance on the entrance aperture of JANUS. We calculate the SPST by ray-tracing for a grid of entrance polar and azimuth angle. For each entrance angle we calculate the SPST irradiance map for the minimum and maximum working wavelengths (340nm and 1080nm) and for expected begin-of-life (BOL) and end-of-life (EOL) contamination levels of the optical surfaces.

### 3.3 Optimizing ray-trace effectiveness

Our model has been optimized to decrease the simulation time required for the calculation of the SPST maps. The strategies adopted are the following ones:

- 1) We make use of the “scatter towards region of interest” functionality of FRED to scatter rays only towards the relevant regions (in general rays are scattered towards the detector or its image through the optics).
- 2) We consider only up to second-order scattering paths by terminating rays with more than two scattering or ghost-reflection bounces
- 3) We set the number of scattered rays of every component in a way that every stray-light path is sufficiently sampled (10 rays per pixel approximately) on the detector, thus increasing the number of scattered rays for surfaces with small area, like the edges of the diaphragms on the external baffle. This is crucial to avoid paths generating just a few bright pixels on the SPST map.
- 4) We use a detector with reduced resolution. The pixel size is approx. 60 $\mu$ m against the 7 $\mu$ m of the real detector. This assumption is good as long as all the stray-light features are bigger than the pixel size.
- 5) We perform a multiple step ray-trace: a first ray-trace is used to identify the most critical paths (i.e. those paths that generates 90% of the total stray-light power on the detector) for a given illumination angle. The number of rays used for this preliminary step should be enough to ensure a proper determination of the average power of each path, even if the power is distributed only on a few pixels. Once the most critical paths have been identified, we trace much more rays through the system one step at a time and we terminate the rays not

following the worst paths. The second step allows to trace a denser grid of rays and get a better ray statistic on the detector while keeping simulation time reasonable. This step is necessary to get smooth irradiance maps.

All these procedures are controlled by script (written in the FRED scripting language) in a way that parameters can be fine-tuned several times just by changing the simulation input values.

## 4. RESULTS

### 4.1 Critical paths identification

Most of the critical stray-light paths could be already identified during the first analysis phase, without setting any scattering property to the geometrical model. For each path we identified the most critical illumination directions and studied possible improvements also by aid of a visual representation of the critical rays. An example is provided in Figure 4 where black rays denote illumination from outside and red rays indicate visibility from the detector. In the examples provided below it is visible the direct illumination of the internal chamfer of the primary mirror (left figure) and of the edge thickness of the filter mount (right figure). The result of the preliminary analysis mainly identified first-order stray-light paths intrinsic to the optical configuration and only minor modifications were suggested, like the increase of the chamfer/bevel of some edge surface.

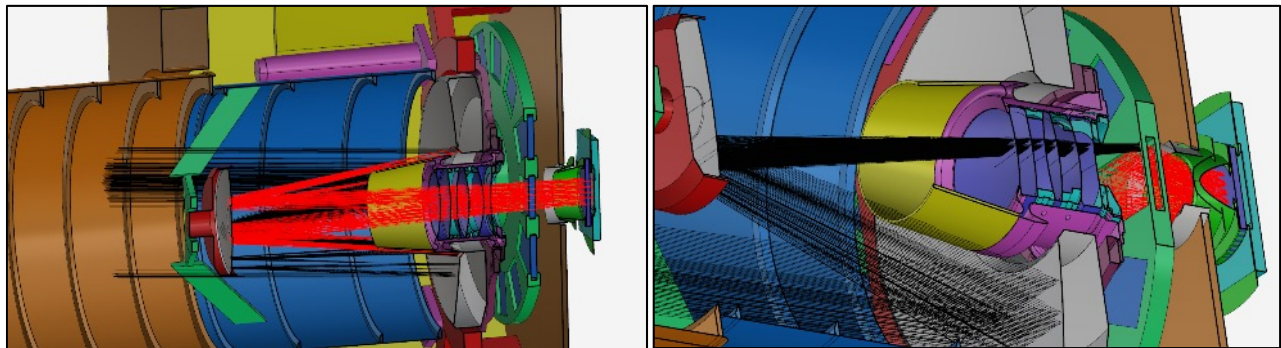


Figure 4. Example of critical paths. Black rays indicate illumination from outside, red rays indicate visibility from the detector. Left: illumination of the internal chamfer of the primary mirror. Right: Illumination of the edge of the filter mount.

### 4.2 SPST maps

The second part of the analysis provides a quantitative evaluation of the stray-light of JANUS and gives the relative contribution of the different stray-light sources. In particular, for in-field illumination the stray-light is dominated by ghost reflections of the detector window, the science filters and the field corrector; for sources close to the field of view most of the stray-light is produced by scattering of surfaces close to the optical path (filter mount, lens spacers, M2 mount) or by the micro-roughness of the mirrors; for sources at a polar angle  $>15^\circ$ , scattering from the external baffle is the strongest contributor to stray-light, in particular that produced by the edge thickness of the diaphragms. As an example, Figure 5 shows the SPST irradiance map relative to four different illumination angles in logarithmic color scale. In the top-left map, ghost reflections are clearly visible, while for out-of-field illumination the maps are smoother except for some effect of baffle shadowing visible in the bottom-right figure.



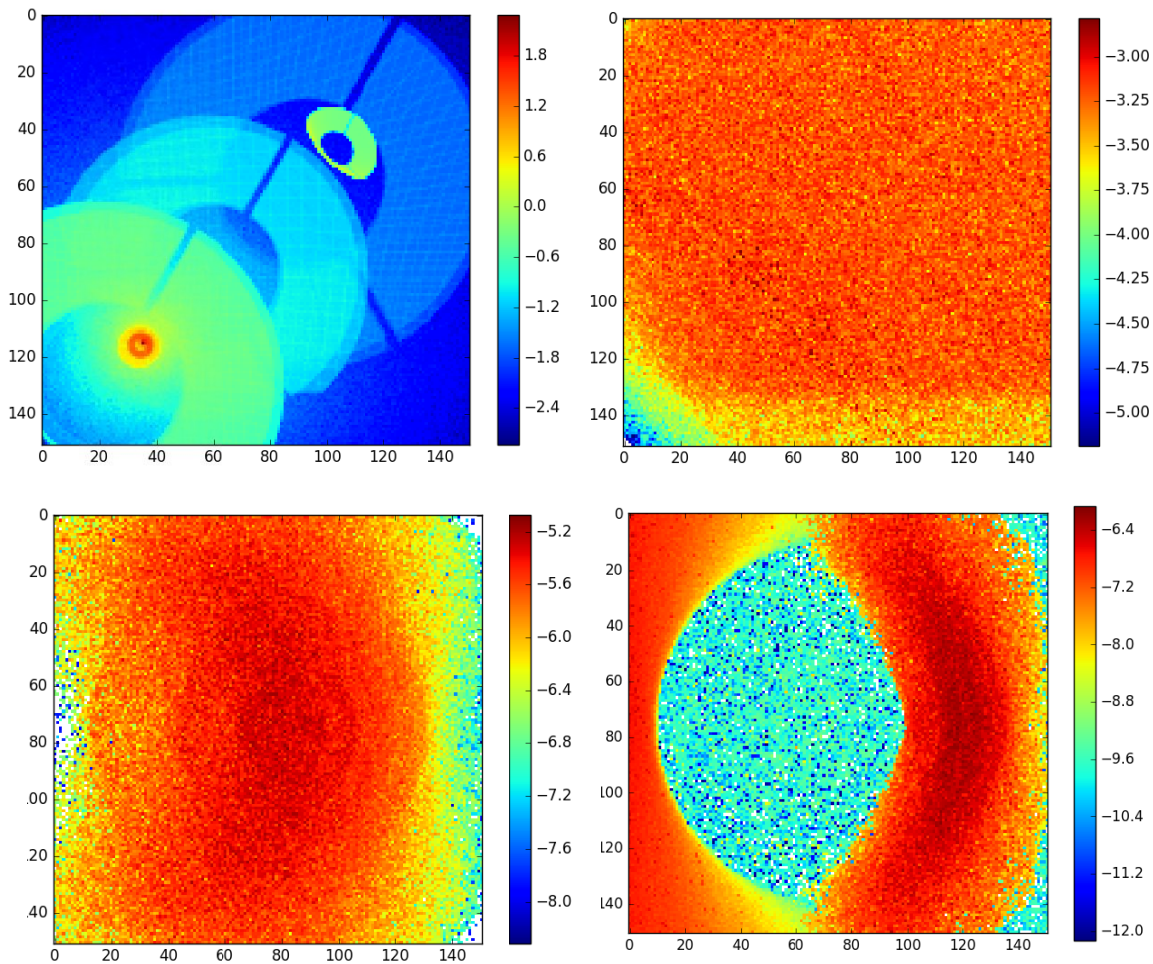


Figure 5. Examples of SPST irradiance maps in logarithmic color scale. Polar angle of illumination are respectively:  $0.8^\circ$  (top-left),  $5^\circ$  (top-right),  $35^\circ$  (bottom-left),  $55^\circ$  (bottom-right).

### 4.3 Application to a general illuminating geometry

The SPST maps calculated above only give the stray-light generated by a point source at infinity. In a real and more general case, stray-light will strongly depend on the illumination geometry and JANUS will actually observe extended objects for most of the mission.

Under the assumption that the stray-light distribution on the detector generated by an extended object will smear-out the localized features of the SPST maps, the mean value of the SPST at a given direction can be considered to be representative of the stray-light irradiance for that given direction. This quantity is simply called Point Source Transmittance (PST) since the “spatial” information is discarded. In the case of JANUS, the PST curve as a function of the polar angle with respect to the boresight is a monotonically decreasing function as shown in Figure 6. The four colors in figure denote the PST for the minimum and maximum wavelength and for “begin-of-life” and “end-of-life” level of contamination of the optics.

The knowledge of the PST allows to estimate the stray-light in a general illumination scenario by integrating it over the solid angle subtended by the light source. Integration is done by linearly interpolating the PST between the simulated data-points. In the case of simple illumination geometries, the total stray-light can be derived in a semi-analytical way<sup>12</sup>, while for more general geometries a numerical integration is necessary. We are currently developing a python routine to evaluate the ratio between the total stray-light and the scientific signal for any given observing scenario. This will allow us to check the instrument performance and compare it with the requirements.

In the python script it is possible to define several objects in the 3D space, each object characterized by dimension, position and BRDF. A point-like source (the Sun) is added in the scene, objects are illuminated by it and scatter in the instrument.

3D space in front of the instrument is sampled in angular space (polar and azimuth angles); for each sample is determined which object is seen by the instrument pupil and its input irradiance; consequently stray-light signal and scientific signal per pixel are calculated. At the moment the script implements only spheres and lambertian BRDFs, but possible extensions are ‘quasi-trivial’. The script may be fed with CSV files with coordinates of objects at different time, so to evaluate evolution of signal and stray-light with cruise.

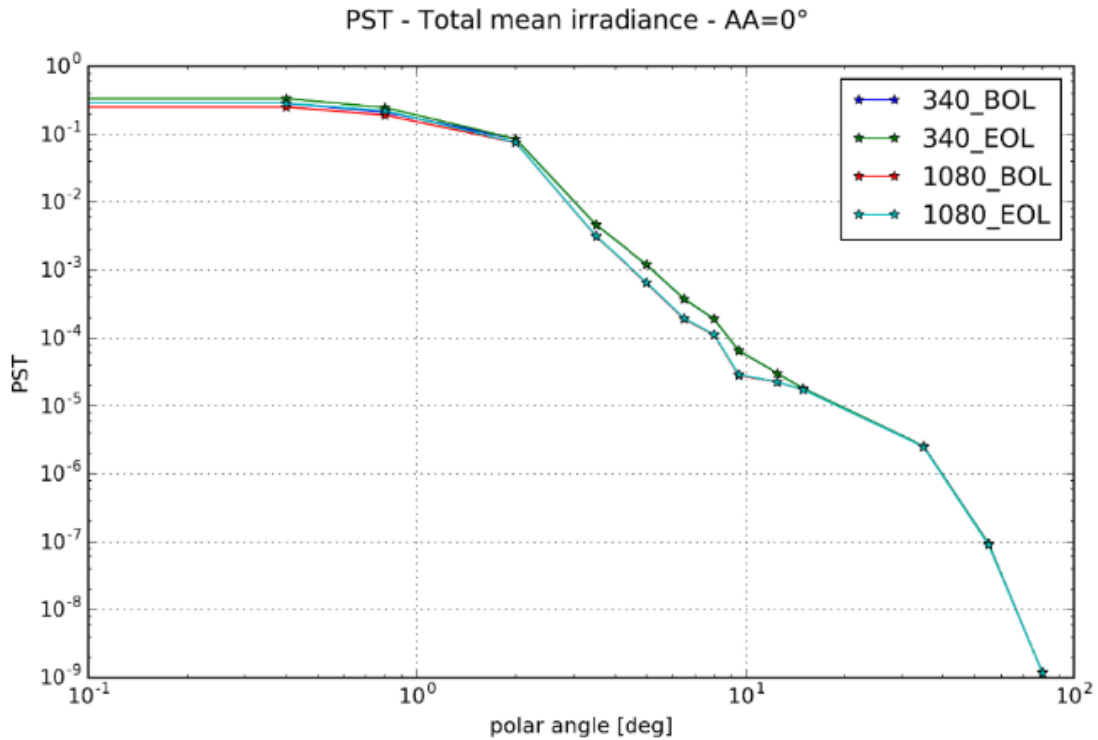


Figure 6. Total PST (mean irradiance over the detector) as a function of polar angle for the different wavelengths and contamination conditions.

## 5. ACKNOWLEDGMENTS

This study was supported by the Italian Space Agency (ASI) – Contract number: 2013-056-RO

## REFERENCES

- [1] Grasset, O., et al., “Jupiter Icy moons Explorer (JUICE): an ESA mission to orbit Ganymede and to characterize the Jupiter system”, Planet and Space Sci. 78, 1-21 (2013)
- [2] Witasse, O., Altobelli, N., Barabash, S., et al., “JUICE: A European Mission to Jupiter and its Icy Moons”, EPSC 2015-564 (2015)

- [3] Della Corte, V., Schmitz, N., Zusi, M., Castro, J. M., Leese, M., Debei, S., Magrin, D., Michalik, H., Palumbo, P., et al., "The JANUS camera onboard JUICE mission for Jupiter system optical imaging", Proc. SPIE, 9143, 914331 (2014)
- [4] Palumbo, P., Jaumann, R., Cremonese, G., et al., "JANUS: The Visible Camera Onboard the ESA JUICE Mission to the Jovian System", Lunar and Planetary Science Conference, 45, 2094 (2014)
- [5] Bruzzone et al., "The Radar for Icy Moon Exploration (RIME) on the JUICE Mission", AGU Fall Meeting Abstracts, P53G-01 (2015)
- [6] Cofano, A., Komatsu, G., Pizzi, A., et al., "Ganymede's Surface Investigation in Support of the Radar for Icy Moon Exploration (RIME) Instrument", Lunar and Planetary Science Conference, 46, 1382 (2015)
- [7] Greggio, D., Magrin, D., Munari, M., et al., "Trade-off between TMA and RC configurations for JANUS camera", Proc. SPIE, 9904, 990451 (2016)
- [8] Marra, G., Colangeli, L., Mazzotta Epifani, E., et al., "The Optical Design of the High Resolution Imaging Channel for the SIMBIO-SYS experiment on the BepiColombo Mission to Mercury", Memorie della Societa Astronomica Italiana Supplementi, 12, 77 (2008)
- [9] Cessa, V., Beck, T., Benz, W., et al., "CHEOPS: a space telescope for ultra-high precision photometry of exoplanet transits", SPIE Conference Series, 10563, 105631L (2017)
- [10] Beck, T., Gambicorti, L., Broeg, C., et al., "The CHEOPS (characterising exoplanet satellite) mission: telescope optical design, development status and main technical and programmatic challenges", SPIE Conference Series, 10562, 1056218 (2017)
- [11] Soman, M., Holland, A.D., Stefanov, K.D., et al., "Design and characterisation of the new CIS115 sensor for JANUS, the high resolution camera on JUICE", Proc.SPIE, 9154, 915407 (2014)
- [12] Greggio, D., Magrin, D., Munari, M., Zusi, M., et al., "Optical design and stray light analysis for the JANUS camera of the JUICE space mission", Proc. SPIE, 9626, 96263J (2015)